

# An explainable semi-personalized federated learning model

Konstantinos Demertzis<sup>a,\*</sup>, Lazaros Iliadis<sup>b</sup>, Panagiotis Kikiras<sup>c</sup> and Elias Pimenidis<sup>d</sup>

<sup>a</sup>*School of Science and Technology, Informatics Studies, Hellenic Open University, Greece*

<sup>b</sup>*School of Civil Engineering, Democritus University of Thrace, Kimmeria, Xanthi, Greece*

<sup>c</sup>*Department of Electrical and Computer Engineering, University of Thessaly, Volos, Greece*

<sup>d</sup>*Computer Science and Creative Technologies, University of the West of England, Bristol, UK*

**Abstract.** Training a model using batch learning requires uniform data storage in a repository. This approach is intrusive, as users have to expose their privacy and exchange sensitive data by sending them to central entities to be preprocessed. Unlike the aforementioned centralized approach, training of intelligent models via the federated learning (FEDL) mechanism can be carried out using decentralized data. This process ensures that privacy and protection of sensitive information can be managed by a user or an organization, employing a single universal model for all users. This model should apply average aggregation methods to the set of cooperative training data. This raises serious concerns for the effectiveness of this universal approach and, therefore, for the validity of FEDL architectures in general. Generally, it flattens the unique needs of individual users without considering the local events to be managed. This paper proposes an innovative hybrid explainable semi-personalized federated learning model, that utilizes Shapley Values and Lipschitz Constant techniques, in order to create personalized intelligent models. It is based on the needs and events that each individual user is required to address in a federated format. Explanations are the assortment of characteristics of the interpretable system, which, in the case of a specified illustration, helped to bring about a conclusion and provided the function of the model on both local and global levels. Retraining is suggested only for those features for which the degree of change is considered quite important for the evolution of its functionality.

**Keywords:** Decentralized learning, federated learning, privacy-preserving architecture, explainable AI, local and global interpretability, shapley values, lipschitz constant

## 1. Introduction

The complete transformation of supply chain (SC) in a truly integrated and fully automated process assumes the continuous and endless collection of digital information from every stage of the production [1]. Following this idea, the history of services and products per stage of the supply chain, can be investigated. The emerging continuous need of connectivity, raises serious concerns for the protection of personal data and for digital security as a whole [2].

At the same time, the heterogeneity of the systems included in the supply chain as well as the non-

conventional interoperability, in terms of hardware and software, results to even more serious concerns related to the security and protection of these systems [3,4].

Recently, the authors developed and presented a specialized and technologically up-to-date framework for the protection of digital security, privacy and industrial confidentiality. Specifically, the developed framework is related to an advanced *adaptive federated auto metalearning* mechanism (AFAMM), which operates on a blockchain and applies advanced encryption techniques, to fully ensure privacy and industrial secrecy [5]. The security and privacy focused architecture of this framework, has three main characteristics, namely: a) no sensitive data is transmitted through communication channels b) the data is not stored in a central point of attack and c) the learning algorithms are constantly upgrading their predictability [2,5].

\*Corresponding author: Konstantinos Demertzis, School of Science and Technology, Informatics Studies, Hellenic Open University, Greece. E-mail: demertzis.konstantinos@ac.eap.gr

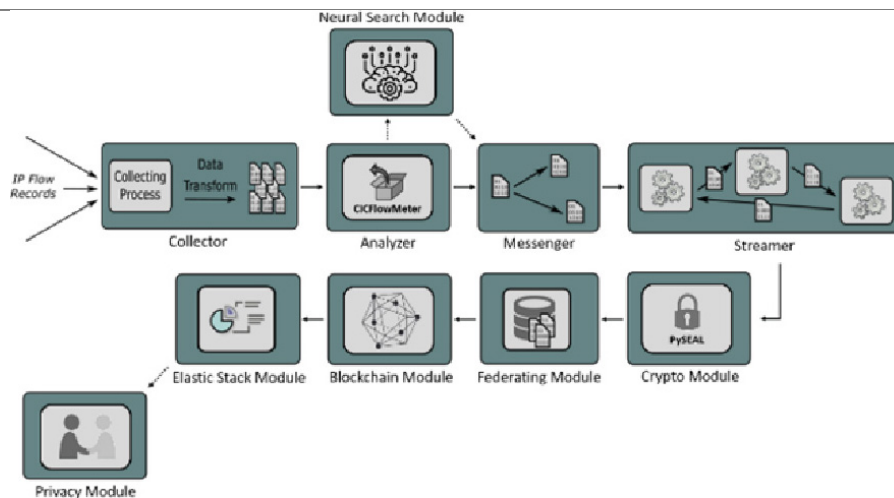


Fig. 1. The blockchain adaptive federated auto meta-learning architecture.

An intelligent control mechanism has been developed to detect malfunctions in the processes of a communication network running under an Industry 4.0 environment [6]. This system is based on the analysis of network traffic and on the development of an automatic intelligent neural network for the control and detection of abnormalities. The training and updating of the model were performed using federated learning and the communication of all involved parts was done through blockchain methods. The modules of this architecture are illustrated in Fig. 1.

Under this framework, when a device wants to communicate with another, the proposed intelligent mechanism is activated, implementing a network traffic control to detect anomalies. In the first phase, the features of the network's traffic are exported in order to form the input vectors to a Neural Network (NN) that is automatically developed following the *Neural Architecture Search* technique. The model is initially trained on the host server with some initial data, in order for the training process to begin. Then, it is encrypted with homomorphic encryption and it is sent via blockchain (BLCH) to nodes that will use it. The nodes in question receive the model and improve it by exploiting the data at their disposal [7–9]. The obtained enhanced version is encrypted and returned via blockchain to the host server. In this stage, the best models are aggregated, and the weighted average is selected using the *Grid Search Weighted Average Ensemble* method. The final model is returned back to the nodes using BLCH. If the traffic is characterized as normal, further communication is allowed. Otherwise, communication is forbidden and an alarm is sent to the control center, for further analysis of the transaction [10].

The federated module allows remote devices to download and run the original trained machine learning model that is developed by the neural search approach. This is populated with local data, improving its accuracy, and then it is sent back to the federated module, which summarizes the changes using the *Dynamic Weighted Average technique*. The updated version, is fed back to the network nodes, through the blockchain module [11,12].

Based on this architecture, the initial experiments give the impression that there is a continuous improvement of the intelligent model, and that end users can have constant access to an ever-upgraded NN. After extensive observation, it was demonstrated that learning a single universal model by aggregating the best models and selecting the weighted average via Dynamic Weighted Average (DWA), could not satisfy the local needs of the users. This is due to the fact that the events they had to deal with, were significantly different in terms of the data threats they process. For example, mobile users face different threats than the Internet of Things' (IoT) devices or SCADA industrial network terminals [10,13].

While constant upgrade increases generalization, it raises serious concerns for its efficiency at local level. Figure 2 shows the noticeable decrease of the local model's accuracy, compared to the global and to the original ones.

As it can be seen after the first 30 iterations, the local model has significantly higher accuracy than the global one. This is explained by the fundamental hypothesis related to the development of any supervised machine learning model (MLM), according to which, the data

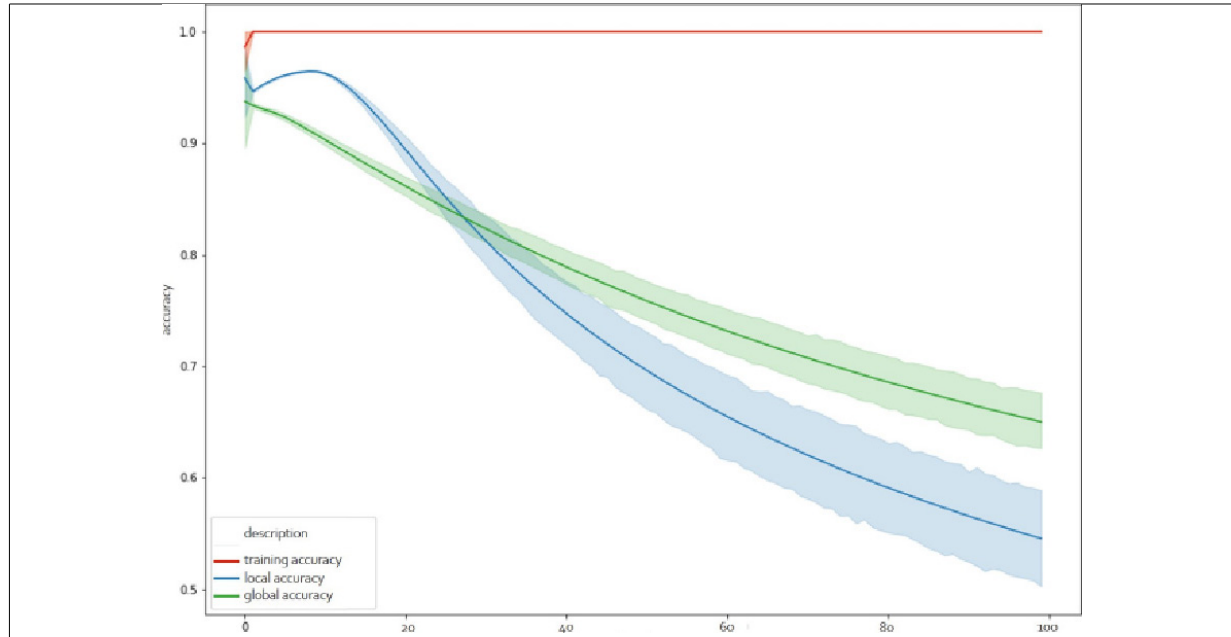


Fig. 2. Local vs global models' accuracy.

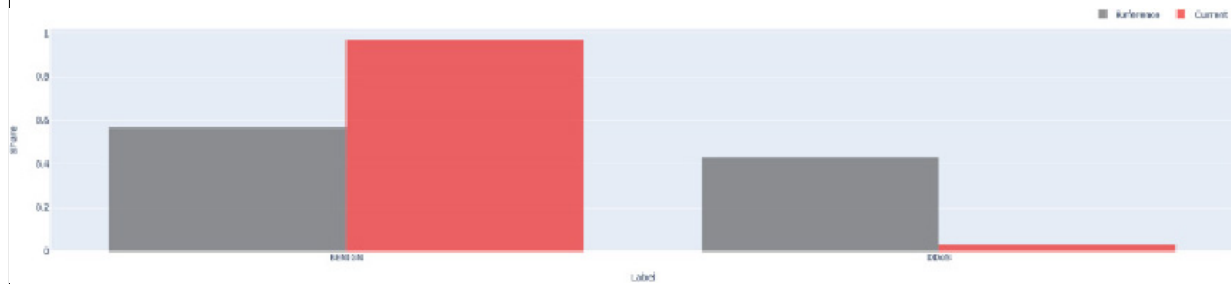


Fig. 3. Drift data by classes.

under consideration, mimic real-world cases. No matter how accurate the MLM, the predictions are correct only if the used data is identical or statistically equivalent to the training vectors. Minor changes (drifts) that a realistic problem is capable of bringing to the data [14, 15], might result in a reduction of the classification accuracy, as it is shown in Fig. 2.

In this research paper, a drift analysis has been performed to identify the response of local models to changes in the data, and to estimate how they affect the properties of the classes that the learning system is trying to discover. In cases where changes occur (drift) a sensitivity analysis can provide accurate information about the quality of the universal model, produced by the federated learning system [16].

Initially,  $p$ -values [17] were calculated to detect changes in the data and to estimate how likely is that the

data will not change (null-hypothesis). The resulting  $p$  values for each feature were less than 0.05, which proves strong evidence against null-hypothesis, as there is less than a 5% probability that null-hypothesis is correct. Therefore, the null-hypothesis is rejected, and an alternative hypothesis is adopted, i.e., that there is a drift in our data. To this regard, the Exponentially Weighted Moving Average (EWMA) algorithm was used, which renews the estimation of a variable by combining the most recent estimates of all previous measurements based on the following Eq. (1) [18]:

$$\begin{aligned} X_t &= az_t + (1 - a)X_{t-1} \rightarrow \\ X_t &= X_{t-1} + a(z_t - X_{t-1}) \end{aligned} \quad (1)$$

where  $X_t$  is the moving average,  $z_t$  is the last measurement and  $a$  is the weight in the interval  $[0, 1]$ , given by the last measurement. The target of the algorithm is to

97  
98  
99  
100  
101  
102  
103  
104  
105  
106  
107  
108  
109  
110  
111  
112  
113

114  
115  
116  
117  
118  
119  
120  
121  
122  
123  
124  
125  
126  
127

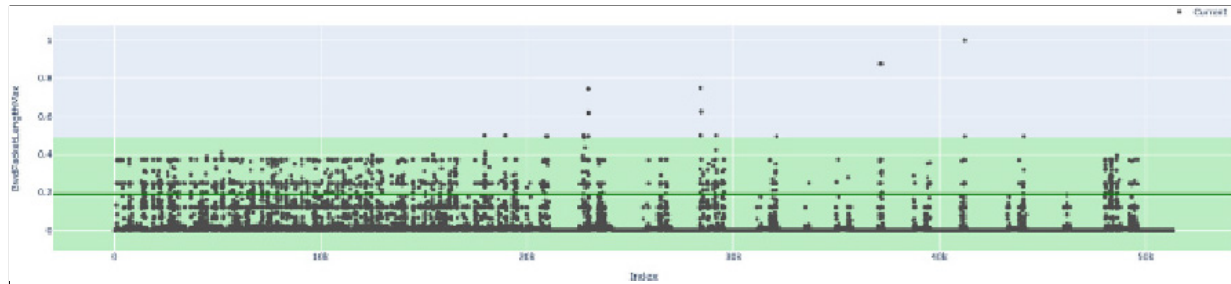


Fig. 4. Drift data in BwdPacketLengthMax future.

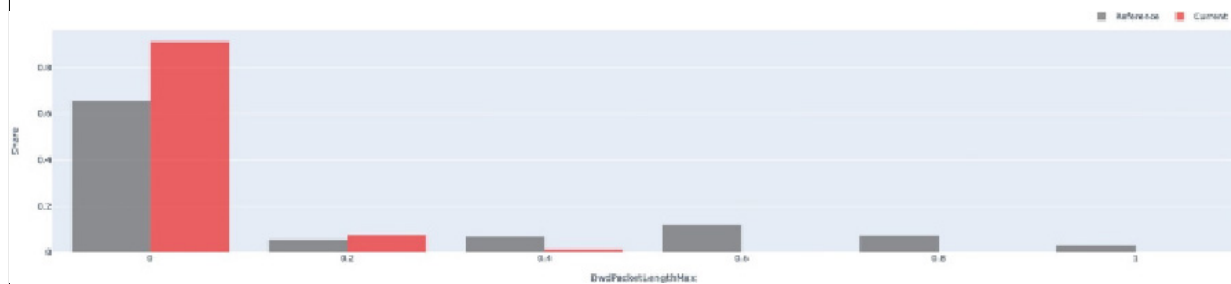


Fig. 5. Drift data in BwdPacketLengthMax future by classes.

generate an estimate that gives more weight to recent measurements, assuming that they are more likely to be relevant. Based on the performed EWMA tests, 95.45% of the dataset's features (63 out of 66) appear to be drifted, as shown in the following Fig. 3.

A specific example of the *BwdPacketLengthMax* feature and its dispersion, appears in the following Figs 4 and 5.

From the above analysis it was concluded that there are three options that can be followed to effectively address the problem [3,18,19]:

1. The first is retraining the system. This approach is characterized by high computational costs that are considered unacceptable, while in practice, this methodology did not perform well.
2. The second is the use of Adaptive Learning methods [20] that are capable to follow changes presented by the data stream. The methodology in question is first checked for the accuracy of the categorization it can produce. It also requires mechanisms that forget outdated examples and therefore address the problem of catastrophic forgetting. Finally, it develops requirements for the model to be reviewed on an ongoing basis, which creates serious computational costs, while its utilization would be preferable for data flow analysis.
3. The third is detecting changes and retraining only those features of the model for which the degree

of change is considered sufficiently significant. The methodology in question, requires strategies to detect and quantify potential changes in the data that modify their distribution over time. It also needs a reliable model for identifying those features of the model that require retraining.

This paper follows the third option as the preferable methodology, in order to explore the personalization potential of federated learning for each user. Thus, only the necessary characteristics of the model are retrained, based on the respective needs and the events that it is called to face.

## 2. Related research

The methodology of the federated learning technique, has been of great interest to the research community. In this section related work will be presented.

For example, in [11] it is presented a comprehensive study with an experimental analysis of federated deep learning approaches for cyber security in IoT applications. Specifically, it is provided an exploratory analysis of federated learning model with three deep learning approaches, namely, Recurrent Neural Network (RNN), Convolutional Neural Network (CNN), and Deep Feed-forward Neural Network (DNN). For each deep learning model, the performance of centralized and federated

128  
129  
130  
131  
132  
133  
134  
135  
136  
137  
138  
139  
140  
141  
142  
143  
144  
145  
146  
147  
148  
149  
150  
151  
152  
153  
154  
155  
156

157  
158  
159  
160  
161  
162  
163  
164  
165  
166  
167  
168  
169  
170  
171  
172  
173  
174  
175  
176  
177  
178  
179  
180  
181

learning under three real IoT traffic datasets is studied. Furthermore, the article aims to provide important information on federated deep learning approaches with emerging technologies for cyber security. In addition, it demonstrates that federated deep learning approaches outperform the classic/centralized versions of machine learning (non-federated learning) in assuring the privacy of IoT device data and providing higher accuracy in detecting attacks.

However, since adversaries can track and derive participants' privacy from the shared gradients, federated learning is still exposed to various security and privacy threats. In [21], the authors consider two major issues in the training process over deep neural networks: 1) how to protect user's privacy (i.e., local gradients) in the training process and 2) how to verify the integrity (or correctness) of the aggregated results returned from the server. Several approaches focusing on secure or privacy-preserving federated learning have been proposed and applied in diverse scenarios to solve the above problems. However, it is still an open problem enabling clients to verify whether the cloud server is operating correctly while guaranteeing users' privacy in the training process. Therefore, a model named VerifyNet is proposed which is a privacy-preserving and verifiable federated learning framework. Specifically, the authors presented a double-masking protocol to guarantee the confidentiality of users' local gradients during the federated learning. Then, a cloud server is required to provide proof about the correctness of its aggregated results to each user. Also, it is claimed that it is impossible that an adversary can deceive users by forging evidence unless it can solve the NP-hard problem adopted in their model. In addition, VerifyNet is also supportive of users dropping out during the training process. The extensive experiments conducted on real-world data also demonstrate the functional performance of the proposed scheme.

Due to lacking effective incentives and trust, data from different operators cannot be shared directly. In [22], the authors proposed an approach on blockchain-based federated learning for implementing asynchronous collaborative machine learning between distributed agents that own data. This method performs distributed machine learning without a trusted central server. The blockchain smart contract is used to realize the management of the entire federated learning. Using the historical data collected from real systems, the learning agent in the federated learning method adopts a support vector machine (SVM) based, intelligent control model. The authors optimize classic SVM, by assigning

different penalty factors to the majority and minority classes to deal with the imbalanced data. The data sets are mapped to a high dimension using kernel functions to make it linearly separable. Also, they construct a mixing kernel function composed of polynomial and radial basis function (RBF) kernel functions, which uses a dynamic weight factor to improve the model accuracy. The simulation results demonstrate the efficiency and accuracy of their proposed intelligent control method.

On the other hand, because the outcomes of attack detection are critical to cybersecurity, every decision should be supported by compelling arguments. Deep learning methods can extract valuable features directly from original data. However, this model is complex and considered a "black box," resulting in low model interpretability. As a result, interpretability has become a bottleneck for deep learning methods used in attack detection. The authors of [23] proposed a deep learning method that can be interpreted based on spatial domain attention. The model can detect and locate feature strings in packets, providing a meaningful semantic explanation for the detection results. The authors conducted qualitative and quantitative experiments on the following datasets DARPA1998, UNSW-NB15, and CIC-IDS-2017. The experimental results show that our method's interpretability outperforms state-of-the-art interpretable models in quantifiable criteria while retaining comparable classification accuracy.

In addition, to balance Transient Stability Assessment (TSA) accuracy and transparency, this paper [24] proposes an interpretable DL-based TSA model. The proposed method combines a deep neural network's strong nonlinear modeling capability with the interpretability of a Decision Tree (DT). The proposed interpretable DL-based TSA method can visually explain the TSA decision-making process by regularizing the DL-based model with the average DT path length during the training process. The simulation results show that the proposed method can produce highly accurate TSA results and interpretable TSA decision-making rules, which can be used to design preventive control actions.

Finally, the feed forward (FF) designed convolutional neural network (FF-CNN) is a network that can be interpreted. The model's parameter training does not necessitate backpropagation (BP) or Stochastic Gradient Descent optimization algorithms (SGD). The entire network is built on the previous layer's statistical data, and the current layer's parameters are obtained in a single pass. Because FF design reduces network complexity compared to the BP algorithm, FF-CNN outperforms

the BP training method in semi-supervised learning, ensemble learning, and continuous subspace learning. However, the FF-CNN training process or model release results in leakage of training data privacy. The authors of this paper [25] analyze and demonstrate that an attacker can obtain the private information of the original training data after mastering the FF-CNN training parameters and partial output responses. As a result, training in data privacy protection is critical. However, because of the unique characteristics of the FF-CNN, existing deep learning privacy protection technology is inapplicable. To protect the training data in FF-CNN, the authors are proposing a differential privacy subspace approximation technique with adjusted bias (DP-Saab). They design the privacy budget allocation based on the ratio of the eigenvalues and allocate a larger privacy budget to the filter with a significant contribution, and vice versa, based on the different contributions of the model filters to the output response. Extensive experiments on MNIST, Fashion-MNIST and CIFAR-10 datasets show that the DPSaab algorithm outperforms existing privacy protection technologies in terms of utility.

### 3. Methodology

The proposed methodology uses Shapley Values [26, 27] to generate global and local interpretabilities capable of explaining why the model reaches a specific decision. Respectively, it can detect how the Lipschitz Constant [28,29] evolves during the training of the individual characteristics of the intelligent model, in order to evaluate the methodology [30,31].

Thus, by combining these two methods, a completely transparent model is realized, capable to reveal the following [32]:

- a) the actual source of the data; b) the implemented training strategy; c) the type of the employed intelligent model; d) the hyperparameters used for the training and testing data sets; e) the features introduced to the model and the analysis of obvious and hidden existing correlations; f) the characteristics of the model with the highest predictability; g) the influence of each characteristic on the final prediction in both training and testing and in the accurate measurement of the model's performance by evaluating unknown data [33–35].

#### 3.1. Shapley values

A thorough approach using the *Global and Local Interpretability* methodology was performed to obtain a

holistic picture of the network, in terms of how it makes decisions, what are its most important features, and what interactions are taking place between the features in this methodology [36].

Global interpretability provides an overview of the model, while Local interpretability focuses on explanations from a small data area, which analyzes a single instance of the data set and explains why the model has reached a specific decision. This is because in small areas of data, the prediction may depend only linearly or monotonously on certain features of the model, rather than having a more complex dependence on them. Thus, the global and local interpretabilities of the model's features could be identified. Moreover, this could determine the parameters that would be part of the local or the global model [37].

Shapley values are a very effective way of generating explanations on how a model works. Its mathematical background comes from the *Cooperative/Coalitional Game Theory*, where the payoff/gain of a cooperative game's players, is realized by a real function which gives values to sets of players [26].

Specifically, the problem of a neural network's architectural structures is considered as a cooperative game, whose players are the characteristics of the data set, the profit function is the NN' model under consideration, and the predictions are the corresponding winnings [38,39].

In this content, the Shapley values show the contribution of each feature and therefore the explanation why the model made a specific decision.

More specifically, the Shapley value of a NN' characteristic  $i$ , is given by the following relation [26,32,37]:

$$\varphi_i = \sum_{S \in F \setminus \{i\}} \frac{|S|!(M - |S| - 1)!}{M!} [f_{S \cup \{i\}}(x_{S \cup \{i\}}) - f_S(x_S)] \quad (2)$$

where  $F$  is the set of attributes,  $S$  is a subset of  $F$  and  $M = |F|$  the absolute number of attributes. This relation measures the weight of each attribute by calculating its contribution when it is present in the forecast and then subtracts it when it is absent.

More specifically:

1.  $f_{S \cup \{i\}}(x_{S \cup \{i\}})$ : is the output when the  $i^\infty$  characteristic is present.
2.  $f_S(x_S)$ : is the output when the  $i^\infty$  characteristic is absent.
3.  $\sum_{S \in F \setminus \{i\}} \frac{|S|!(M - |S| - 1)!}{M!}$ : is the weighted average of all the potential subsets of  $S$  in  $F$ .

The Shapley method uses the linear correlation of the independent and dependent variables which is measured by calculating the Pearson R correlation table. The proposed architecture, is considering the inability of the Pearson's method to detect nonlinear correlations such as *sinus wave*, *quadratic curve*. It uses the *Predictive Power Score* (PPS) technique to summarize the predictive data between available forecasts [40]. More specifically, it explains how variable A informs variable B, more than variable B informs variable A. Technically, scoring is a measurement in the interval [0, 1] of a model's success in predicting a variable target with the help of an off-sample variable prediction. This practically means that this method can increase the efficiency and transparency of finding hidden patterns in the data, and thus it can facilitate the selection of appropriate prediction variables [41]. The use of the PPS method also focuses on the fact that a local explanation of the model's parameters must be obtained. As a result, this data should be ultimately capable of operating without retraining and of course without being reinforced in the second phase of training. For the calculation of PPS in numerical variables the metric of *Mean Absolute Error* (MAE) was used, which is the measure used for the quantification of the error between the estimated and the observed values. It is calculated by the following formula [17]:

$$MAE = \frac{1}{n} \sum_{i=1}^n |f_i - y_i| = \frac{1}{n} \sum_{i=1}^n |e_i| \quad (3)$$

where  $f_i$  is the estimated value, whereas the  $y_i$  is the actual value. The average of the above absolute differences of these values is defined as the absolute error of their relation  $|e_i| = |f_i - y_i|$ .

Moreover, the  $F_{Score}$  the Recall and the Precision indices were used:

$$F_{Score} = \frac{2TP}{2TP + FP + FN} \quad (4)$$

### 3.2. Lipschitz Constant

*Lipschitz Constant* (LIPC) [28] was used to evaluate and confirm the final efficiency of the local model, that was obtained by the application of the Shapley methodology. Using LIPC the behavior of the Scattering Transformation can be studied, when a set with similar inputs are entered as inputs. This transformation can approach the operation of a simple neural network architecture, allowing the study of how neural networks succeed in solving difficult problems that require multistage extraction of features [42,43]. At the

same time, the properties of this transformation can explain the way in which a neural network can achieve immutability in the displacement of the input, as well as in small deformations of the input, as in cases of elastic deformation [29].

Specifically, new inputs are generated, when we add at the input  $h$  a very small change  $p$  which results in a new input  $h + p$ , which is classified differently than the original input, using a properly selected input function  $p$  as follows [32,44]:

$$\|S[m](h + p) - S[m](h)\| \leq \|p\|$$

It turns out that the output for a new variable input is no different from the original input more than  $\|p\|$ . So, if the transformation follows the constraints of the Scattering transformation, i.e.:

$$\sum_{i=1}^N |\hat{\psi}_{(i,j)(\omega)}|^2 \leq \frac{C^2}{N}, |\hat{\phi}_{(\omega)}|^2 \leq C^2 \quad (5)$$

This means, that the  $C$  constant is a determinant of how vulnerable the transformation is to input changes of  $p$ .

As the *Lipschitz constant* determines the classifier's ability to correspond to new inputs, it is proposed its use in order to detect how this constant evolves during the training of a neural network's local parameters [32]. In particular, let the input of a Convolutional Neural Network (CNN) be in the form of a vector. Let  $f(x_{in}, c)$  be the output of the network for class  $c$  and  $x_{in}$  the input. Let  $y_{in}, h_{in}$  two different input vectors with respective output  $f(y_{in}, c), f(h_{in}, c)$  and  $y_{ik}, h_{ik}$  the output of the  $k$ th layer in channel  $i$  for each one of the two inputs. The CNN comprises of convolution layers, pooling layers and ReLU activation functions [45]. Thus, for each of the three layer-types we have [3,19]:

1. Let  $k$  layer be a convolution layer. As we express inputs as one-dimensional vectors, convolution with a two-dimensional core  $\psi_{ijk}$ , connecting  $i$ th output channel with the  $j$ th input channel  $u$ , is done by multiplying the input vector with a table  $A_{ijk}$  that is produced by the initial core such as:

$$x_{ik} = \sum_{j=1}^{N_k} A_{ijk} x_{j(k-1)} \quad i = 1, 2, \dots, M_k \quad (6)$$

where  $N_k$  is the number of the input channels and  $M_k$  is the number of the output channels of the Convolutional layer  $k$ . Thus:

$$\|y_{ik} - h_{ik}\|_2 = \left\| \sum_{j=1}^{N_k} A_{ijk} (y_{j(k-1)} - h_{j(k-1)}) \right\|_2$$

$$\begin{aligned}
& \left\| - \sum_{j=1}^{N_k} A_{ijk} h_{j(k-1)} \right\|_2 \\
& \left\| \sum_{j=1}^{N_k} A_{ijk} (y_{j(k-1)} - h_{j(k-1)}) \right\|_2 \\
& \leq \sum_{j=1}^{N_k} \|A_{ijk} (y_{j(k-1)} - h_{j(k-1)})\|_2 \quad (7) \\
& \leq \sum_{j=1}^{N_k} \|A_{ijk}\|_2 \|y_{j(k-1)} - h_{j(k-1)}\|_2 \quad (13) \\
& \Rightarrow \|y_{ik} - h_{ik}\|_2 \leq \sum_{j=1}^{N_k} \|A_{ijk}\|_2 \|y_{j(k-1)} \\
& \quad - h_{j(k-1)}\|_2
\end{aligned}$$

2. Let  $k$  be the Pooling Layer in which there is no overlapping of the areas:

$$\|y_{ik} - h_{ik}\|_2 \leq \|y_{j(k-1)} - h_{j(k-1)}\|_2 \quad (8)$$

3. Let  $k$  be the ReLU layer, then the output layer has the form:

$$x_{ik} = \begin{bmatrix} x_{ik}(1) \\ x_{ik}(2) \\ \vdots \\ x_{ik}(m) \end{bmatrix} \quad (9)$$

The output  $x_{ik}(t)$  is obtained as follows:

$$\begin{aligned}
x_{ik}(t) &= \max(0, x_{i(k-1)}(t)) \\
\|y_{ik} - h_{ik}\|_2^2 &= \sum_{t=1}^m |\max(0, y_{i(k-1)}(t)) \\
& \quad - \max(0, h_{i(k-1)}(t))|^2 \\
& \leq \sum_{t=1}^m |y_{j(k-1)}(t) - h_{j(k-1)}(t)|^2 \quad (10) \\
& = \|y_{j(k-1)} - h_{j(k-1)}\|_2^2 \\
& \Rightarrow \|y_{jk} - h_{jk}\|_2 \\
& \leq \|y_{j(k-1)} - h_{j(k-1)}\|_2
\end{aligned}$$

where  $|\max(0, \alpha) - \max(0, \beta)| \leq |\alpha - \beta|$ .

Using the above equations, the constant  $L_{ik}$  can be estimated, for which the following condition should be met:

$$\|y_{jk} - h_{jk}\|_2 \leq L_{ik} \|y_{10} - h_{10}\|_2 \quad (11)$$

The constant is defined recursively, as  $L_{ik} = 1$ . For any type of layer, we have the following:

1. Convolution layer:

$$L_{ik} = \sum_{j=1}^{N_k} \|A_{ijk}\|_2 L_{j(k-1)} \quad (12)$$

2. Pooling layer:

$$L_{ik} = L_{i(k-1)} \quad (13)$$

3. ReLU function:

$$L_{ik} = L_{i(k-1)} \quad (14)$$

If the network has  $p$  layers the Lipschitz constant that satisfies the following relation:

$$\|f(y_{in}, c) - f(h_{in}, c)\|_2 \leq L_{cp} \|y_{in} - h_{in}\|_2 \quad (15)$$

Having developed the method for finding a *lipschitz constant* for the network, this research studied how it evolves during the training of a NN.

The following layers were included:

1. Embedding layer with hyperparameters that indicate the dimensions of the emerging integrations.
2. Dropout layer with hyperparameters indicating the dropout rate.
3. 1D Convolution layer with hyperparameters' filters and kernel size that define the number of the output channels and the width of the 1D core respectively.
4. bi-LSTM layer  $\mu\varepsilon$  with hyperparameters that indicate the size of the output dimensions of the lst layer.
5. Dense layer with two outputs and Sigmoid activation function.

This network is characterized by its simplicity, as it uses 1D Convolution and a bi-LSTM layer that are stacked one after the other, in scalable depth. Overall, the hyperparameters of the model are presented below:

1. embedding\_size = [32, 128].
2. dropout = [0.01, 0.1].
3. filters = [16, 32, 64].
4. kernel\_size = [3, 5, 7].
5. pool\_size = [2, 4].
6. lstm\_output\_size = [16, 64].
7. batch\_size = [8, 16, 32].

The network comprises of 5 layers with two different outputs in the last layer, one for each class, namely: *Distributed Denial of Service* (DDoS), and Benign. The average value of the constants  $L_{i5}$  symbolized as  $L_{out}$  was recorded

$$L_{out} = \frac{1}{2} \sum_{i=1}^2 L_{i5} \quad (16)$$



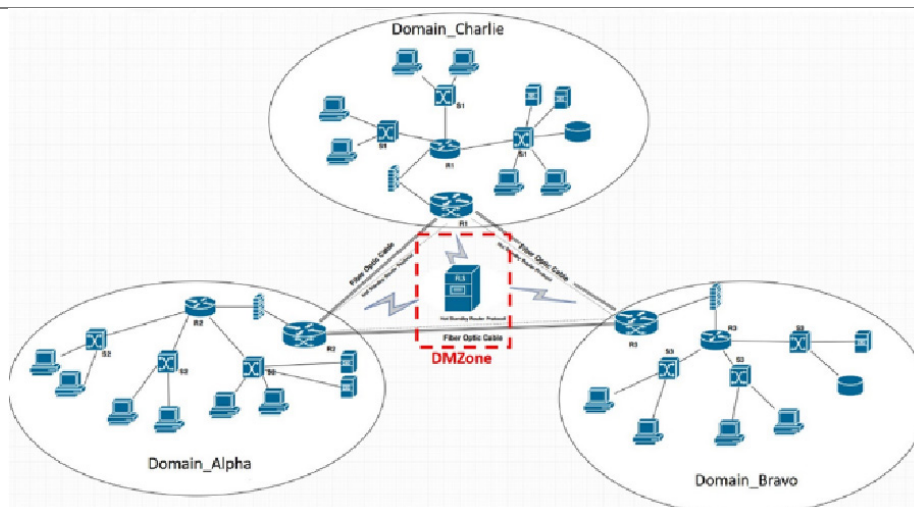


Fig. 6. Architectural modeling of the federated learning partners.

Following the experimental validation of the proposed method, the network was trained using 70% of the available data vectors [46,47]. At the end of each training season, the constant  $L_{out}$  was recorded. The evolution of the NN during the training process was studied thoroughly [48,49]. The hardware used, was based on the GPU chipset, optimized for the free deep learning TensorFlow library.

A collaborative network of three *federated partners* namely: *domain\_alpha*, *domain\_bravo* and *domain\_charlie* that communicate with each other through optical fibers, was simulated in order to implement the Federated Learning (FEL) scenario. The FEL Server (FLS) is located in the Demilitarized Zone (DMZone). Its task is to initiate model's training, with some initial data and to apply the algorithmic process of aggregating the optimal models and selecting the weighted average, via the Dynamic Weighted Average method [2,5,6,9,32]. The overall architecture is presented in Fig. 6.

#### 4. Dataset, scenarios and results

The interconnected heterogeneous industrial systems of specialized mechanical equipment exchange huge amounts of data in the unit of time. The analysis, and classification of data traffic, is one of the most serious tasks for the monitoring of large-scale attacks, as well as for the study of cybercrime [13,16].

The substantive evaluation of the proposed intelligent system was carried out on the *CICDDoS2019* [50], which is one of the most comprehensive web traffic analysis datasets, developed under the supervision of

the *Canadian Institute for Cybersecurity*, with an emphasis on DDoS attacks' detection. The DDoS are very well-organized types of attacks in which the identity of the attacker, remains hidden using the legitimate component of a third party [51].

The set includes modern DDoS attacks, which have been detected in real incidents, and have been identified based on attack indicators. Specifically, the web traffic packages included in this dataset are sent to the *reflector servers* by intruders with source IP address set to target victim IP address, in order to crush the victim's system with response packets.

The attacks are performed through the application layer using transport layer protocols. The malware spectrum includes: TCP-based (*Transfer Control Protocol*) attacks such as MSSQL, SSDP, UDP-based (*User Datagram Protocol*) attacks such as CharGen, NTP, and TFTP, and more complex ones, that can be performed either with TCP or with UDP, such as DNS (*Domain Name Server*), LDAP (*Lightweight Directory Access Protocol*), NETBIOS (Network Basic Input/Output System) and SNMP (*Simple Network Management Protocol*). Moreover, there are TCP based attacks (e.g., MSSQL, SSDP) UDP based ones (e.g., CharGen, NTP and TFTP). More complicated attacks can be executed either via TCP or via UDP, e.g., DNS, LDAP, NETBIOS and SNMP.

There are also UDP flood attacks, where UDP packets are sent at a very high rate to random ports on the victim's system, resulting in depleted network bandwidth, degraded performance, and system crashes.

SYN (short for Synchronization) flood attacks constitute a serious threat, where attackers are forcing the

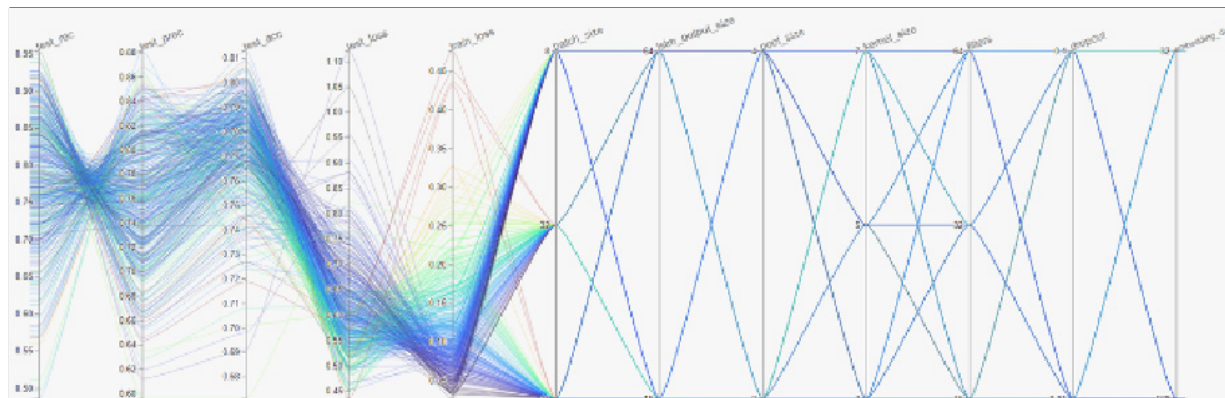


Fig. 7. A parallel coordinates plot developed in the training process (Appendix 1).

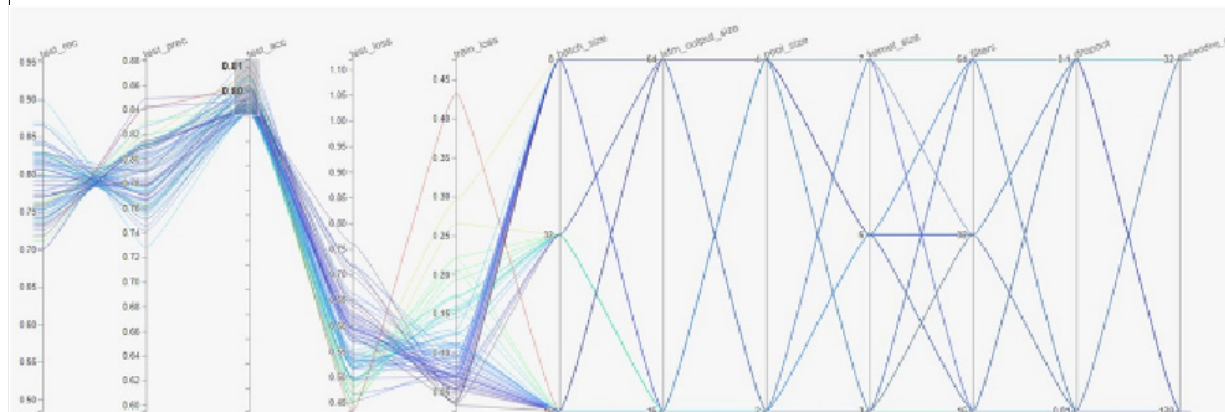


Fig. 8. A parallel coordinates' plot from global interpretabilities.

573 victim's system to consume server resources continu- 593  
574 ously, until it malfunctions or crashes. This is achieved 594  
575 by sending repetitive SYN packets misusing the TCP- 595  
576 three-way handshake. Finally, the set includes UDP- 596  
577 Lag attacks that disrupt the connection between clients 597  
578 and servers using hardware resources or a software pro- 598  
579 gram that runs on the network and uses other users' 599  
580 bandwidth. More details can be found at [51].

581 After data preprocessing, the dataset comprised of 600  
582 66 features, 11,856,972 instances and 2 classes namely 601  
583 Distributed Denial of Service (DDoS) and Benign. Initially, 602  
584 during the training process an attempt was made 603  
585 to interpret the data in their original raw form. Specifi- 604  
586 cally, the diagram of parallel coordinates was employed, 605  
587 to represent the dimensions of the features by parallel 606  
588 axes, one per dimension. Thus, each multivariate point 607  
589 is modeled as a polyline that connects the correspond- 608  
590 ing dimensions. At the same time, this diagram encodes 609  
591 the correlation between the data dimensions, so that 610  
592 the line intersections indicate inverse correlations. The

following figure present a graph of parallel coordinates 593  
during training. 594

595 Extensive tests were performed with data batches, 596  
597 the size of which varied, to identify local interpretabil- 597  
598 ities. Local interpretabilities provide explanations that 598  
599 come from a small data area, which analyzes a rela- 599  
600 tively small batch of data and explains why the model 600  
601 made a specific decision for that particular batch [52]. 601  
602 This is due to the fact that in small areas of data, the 602  
603 prediction may depend only linearly or monotonously 603  
604 on certain features of the model, rather than having a 604  
605 more complex dependence on them [20]. Thus, in this 605  
606 way the global and local interpretabilities of the model's 606  
607 characteristics can be identified. Also, the parameters 607  
608 of the local model can be distinguished from the ones of 608  
609 the global [53]. An example of a graph of parallel co- 609  
610 ordinates during the detection of global interpretabilities, 610  
is shown in the Fig. 8.

611 Unfortunately, there isn't another comparable model 611  
612 to use as a benchmark. Consequently, to avoid bias on 612

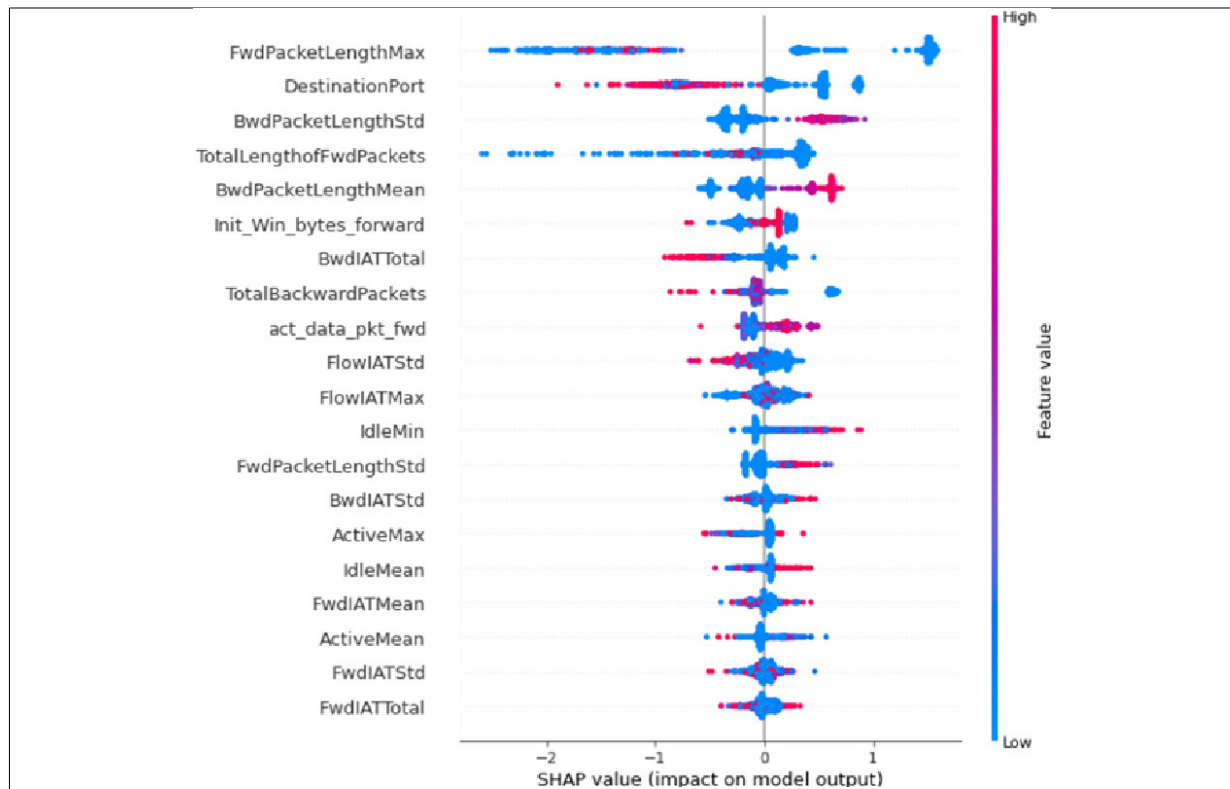


Fig. 9. Summary beeswarm plot.

incorrect impressions, we present the performance of the proposed model without making any comparisons with any other alternative models. The evaluation of the values of the variables in the way they contribute to the prediction and the explanation of each decision of the global interpretabilities, were carried out, using the Shapley values. Figure 9 shows the classification of the records, used in a summary beeswarm plot which is a simple way to capture the relative effect of all the features on the whole data set. Attributes are sorted based on the sum of Shapley values in all samples in the set.

The most important features of the model are shown from top to bottom. Each attribute of the set is symbolized by dots, while the color of the dot symbolizes the value of the attribute (blue corresponds to a low value, while red to a high value). The position of the dot on the horizontal axis depends on its *Shapley value*. It is clear that the attribute *FwdPacketLengthMax* has the most important contribution for the determination of the model's forecasts. The Shapley price is also high for its high values (red dots), so it has a great positive effect globally. In contrast, for low values (blue dots) the Shapley value is low, so it has a negative effect on the

forecast, i.e. it increases the probability that the global model is not affected [54].

An example of a graph of parallel coordinates during local interpretability detection is shown in Fig. 10.

Figure 11, is using a chosen sample from the dataset, in order to represent the typical values of the attributes. Then, ten samples are used to estimate the *Shapley* values for a given prediction. This experiment, requires  $10 \times 1 = 10$  assessments of the model in order to obtain the final conclusion.

This figure shows a local explanation, where the *base\_value* refers to the average value of the model's forecasts, (i.e., in this case the model predicts that the batch of data being analyzed does not affect the local model with a probability of 7%). For this package, the forecast price is 95.92%, so the Shapley prices show the change from the average forecast to the specific forecast. The red arrows push the prediction to the right, that is, they help to increase the probability that the local model will be affected in the specific batch of data, while the blue arrows push to the left, helping to reduce the corresponding probability.

The length of each arrow symbolizes the magnitude of the respective effect on the prediction.

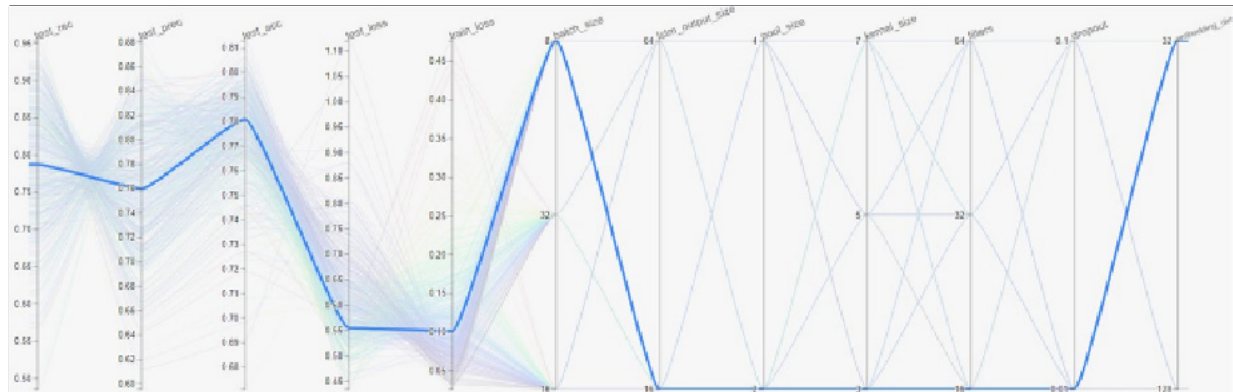


Fig. 10. A parallel coordinates plot from local interpretabilities.



Fig. 11. Explanation of a single prediction-10 evaluations.

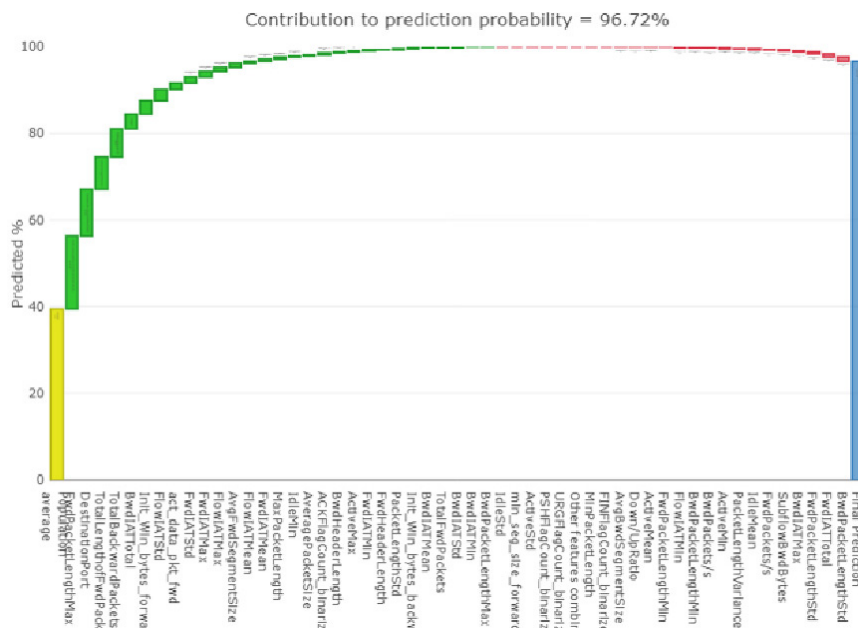


Fig. 12. Partial dependence plot.

661 After the global and local interpretabilities were identified, *Partial Dependence Plots* (PDPs) were used to  
 662 confirm the process, showing the marginal effect that each characteristic has on the predicted result of the  
 663 model. A typical example of the process is shown in Fig. 12.  
 664  
 665  
 666

The number of input features of interest must be limited (usually to one or two in order to accommodate the  
 limitations of human perception); As a result, the input features of interest are typically selected among the  
 essential features. Figure 13 depicts a one-way partial dependence plot for the dataset under consideration.

667  
 668  
 669  
 670  
 671  
 672

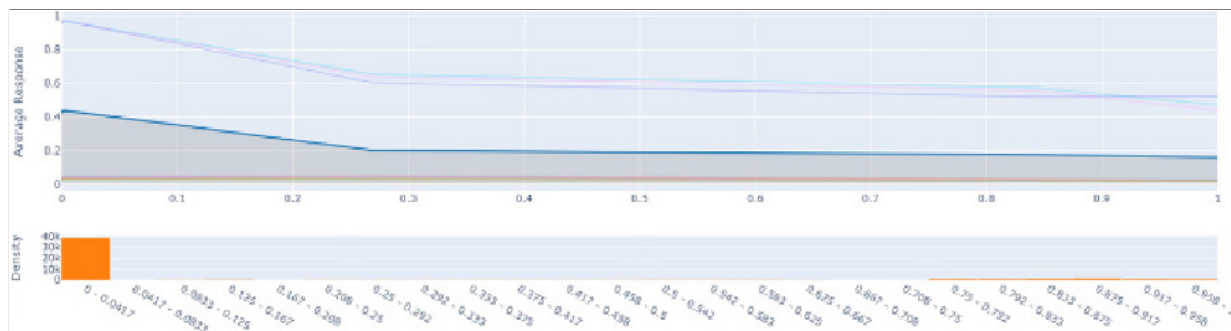
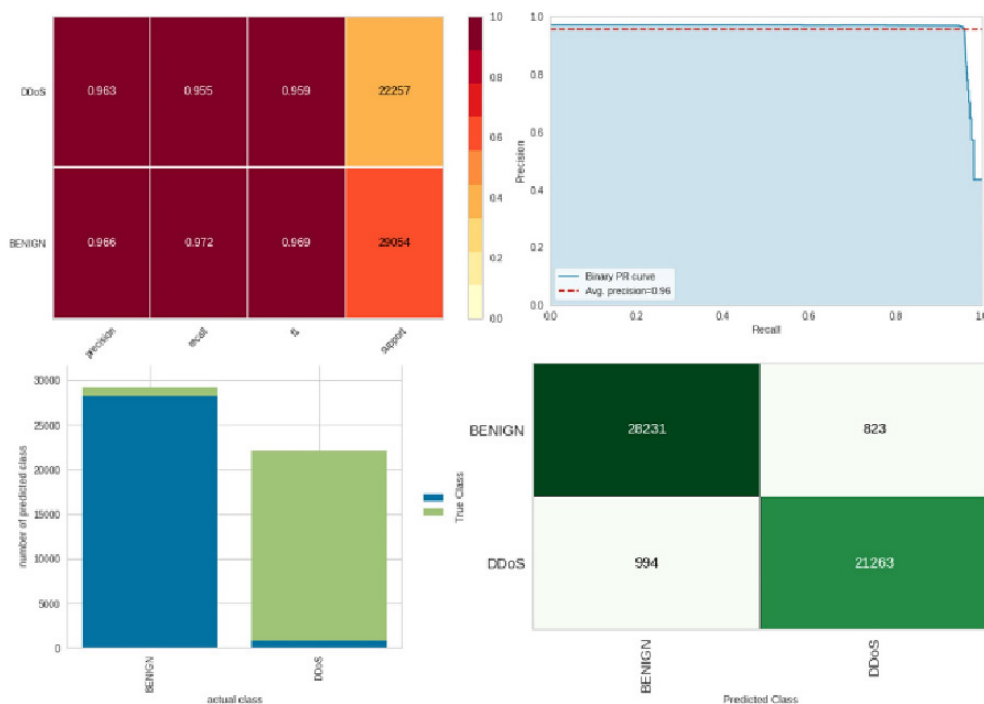
Fig. 13.  $L_{out}$  plot from three federated partners.

Fig. 14. Performance evaluation of federated partner domain\_charlie\_I.

673 One-way dependence plots provide information  
 674 about the interaction between the target response of a  
 675 particular input and a feature of interest (e.g., linear,  
 676 non-linear). The contribution to the prediction proba-  
 677 bility is depicted in the above figure. When the average  
 678 prediction accuracy is 96.7%, we can see a linear rela-  
 679 tionship. In a similar manner, we could investigate the  
 680 impact of various dataset parameters. As a result, these  
 681 interpretations are marginal, considering each feature  
 682 one at a time.

683 Finally, the results of  $L_{out}$  while testing federated  
 684 partners using local and global models are presented in  
 685 the diagram of Fig. 13.

686 The  $L_{out}$  can be an essential importance measure and  
 687 it defined as the deviation of the value of each unique  
 688 feature from the average curve:

$$I(x_S) = \sqrt{\frac{1}{K-1} \sum_{k=1}^K \left( \hat{f}_S(x_S^{(k)}) - \frac{1}{K} \sum_{k=1}^K \hat{f}_S(x_S^{(k)}) \right)^2} \quad (17)$$

689 The  $x_S^{(k)}$  are the  $k$  unique values of feature  $x_S$ .

690 Respectively, the results of the federated partner of  
 691 domain\_charlie are presented in the Figs 14 and 15.

692 Each figure is a summary of prediction results on  
 693 the classification problem. The correct and incorrect

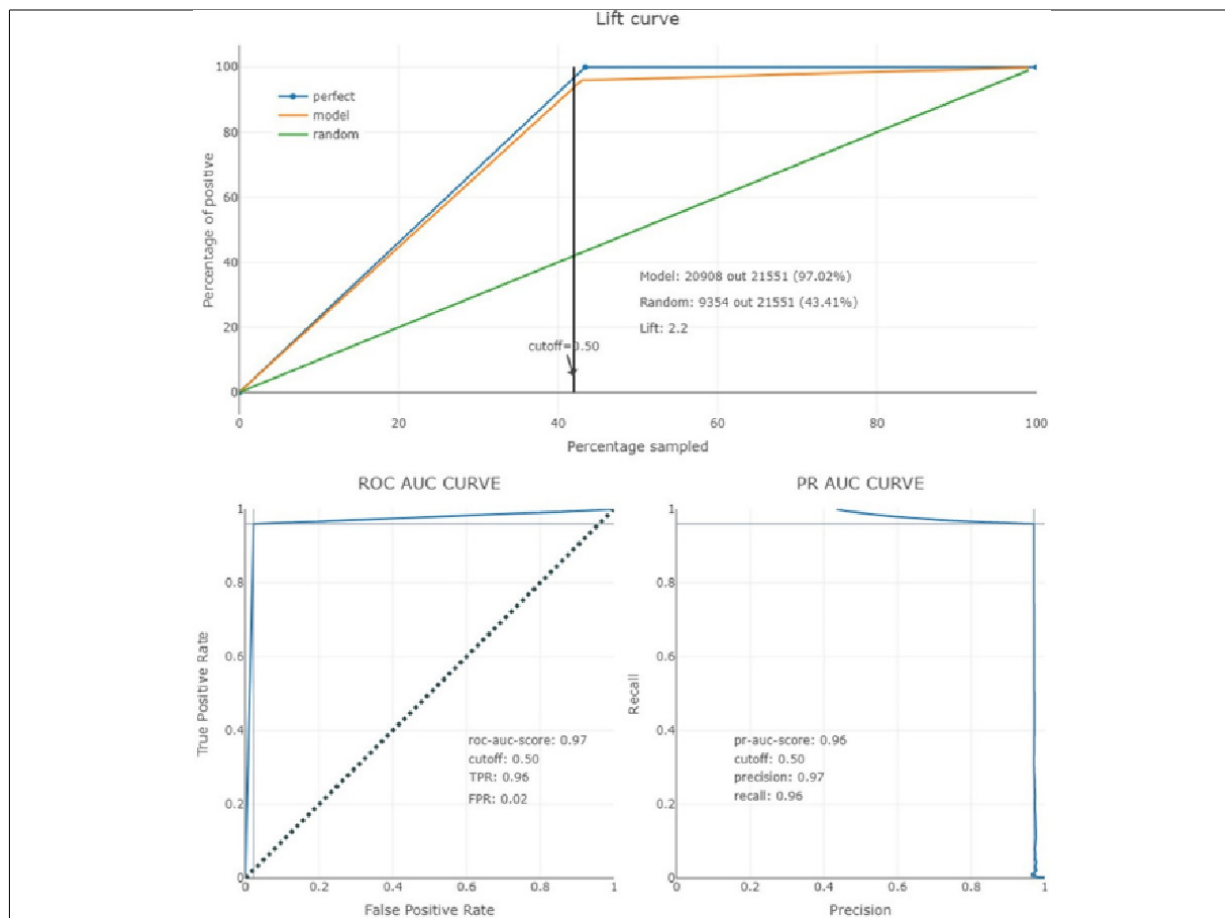


Fig. 15. Performance evaluation of federated partner domain\_charlie\_II.

694 predictions are summarized with count values and they  
 695 are broken down by each class.

696 Furthermore, the precision for each class is the num-  
 697 ber of true positives (i.e., the number of items correctly  
 698 labeled as belonging to the positive class) divided by  
 699 the total number of elements labeled as belonging to  
 700 the positive class (i.e., the sum of true positives and  
 701 false positives, which are items incorrectly labeled as  
 702 belonging to the class). Furthermore, in this context, re-  
 703 call is defined as the number of true positives divided by  
 704 the total number of elements that belong to the positive  
 705 class (i.e., the sum of true positives and false negatives,  
 706 which are items that were not labeled as belonging to  
 707 the positive class but should have been).

## 708 5. Conclusion

709 In this work a novel hybrid explainable semi-  
 710 personalized federated learning model was proposed,

711 utilizing the *Shapley Values* and *Lipschitz Constant*  
 712 techniques to create personalized intelligent local mod-  
 713 els. This is achieved based on the needs and events that  
 714 each user is required to address locally. In particular,  
 715 the system in question provides clear explanations as  
 716 to why the model made a specific decision on locally  
 717 handled data. Then, it detects how the training of the  
 718 intelligent model evolves, by dictating the hyperparam-  
 719 eters that should be trained locally. This results in a  
 720 model that responds optimally to the local problems it  
 721 is called to face.

722 This cutting-edge research proposal has never been  
 723 proposed before in the relevant literature, and we be-  
 724 lieve that it has the potential to considerably extend  
 725 the state-of-the-art in the field of explainable artificial  
 726 intelligence.

727 As demonstrated experimentally with this technique,  
 728 an understanding is gained of how the model makes  
 729 decisions and what interactions are performed between  
 730 the features used, in order to achieve correct or incorrect

classification. The model provide information about the interaction between the target response of a particular input and a feature of interest. Respectively, it allows for the personalization of the federated learning model for each user, so that only the necessary characteristics of the model are retrained, based on the respective needs and the events that it is called to respond. Thus, it offers the ability to manage, control and explain how to handle multiple intermediate representations, as well as more advanced features that may be related to the hierarchical organization of a neural system.

The progressive classification and investigation of the intermediates of the input data along the levels of the hierarchical architecture, even if all the levels share the same weight values, creates clear indications – evidence of how the final decision is made. The combination of Lipschitz and Shapley clearly captures the transitions of internal representations of input signals, even for problems that require long internal memory intervals. The proposed system achieves a result with high accuracy with a white-box algorithm that is interpretable in itself. This is especially important in domains like medicine, defense, finance, and law where it is crucial to understand the decisions and build up trust in the algorithms.

This uniqueness methodology focuses mainly on the development of an automated optimization of the appropriate parameters, so that an even more efficient, accurate and faster explanation process is achieved, in a simple and robust way. Additionally, this paper proposes the utilization of the introduced hybrid technology [55] in recommendation systems, in a completely clear and transparent way. Finally, it would be important to study in the future, the expansion of this system for the implementation of a real-time data flow control framework.

## References

- [1] Sulaiman S, Aldeehani A, Alhajji M, Aziz FA. Development of integrated supply chain system in manufacturing industry. *J Comput Methods Sci Eng*. 2021 Jan 1; 21(3): 599-611.
- [2] Demertzis K, Iliadis L, Pimenidis E, Tziritas N, Koziri M, Kikiras P, et al. Federated Blockchain Supply Chain Management: A CyberSecurity and Privacy Framework. In: Maglogiannis I, Macintyre J, Iliadis L, editors. *Artificial Intelligence Applications and Innovations*. Cham: Springer International Publishing; 2021; pp. 769-79. (IFIP Advances in Information and Communication Technology).
- [3] Alzubaidi L, Zhang J, Humaidi AJ, Al-Dujaili A, Duan Y, Al-Shamma O, et al. Review of deep learning: concepts, CNN architectures, challenges, applications, future directions. *J Big Data*. 2021 Mar 31; 8(1): 53.
- [4] Azan Basallo Y, Estrada Senti V, Martínez Sanchez N. Artificial intelligence techniques for information security risk assessment. *IEEE Lat Am Trans*. 2018 Mar; 16(3): 897-901.
- [5] Demertzis K, Iliadis L, Pimenidis E, Tziritas N, Koziri M, Kikiras P. Blockchain Adaptive Federated Auto MetaLearning BigData and DevOps CyberSecurity Architecture in Industry 4.0. In: Iliadis L, Macintyre J, Jayne C, Pimenidis E, editors. *Proceedings of the 22nd Engineering Applications of Neural Networks Conference*. Cham: Springer International Publishing; 2021. p. 345-63. (Proceedings of the International Neural Networks Society).
- [6] Demertzis K, Iliadis L, Tziritas N, Kikiras P. Anomaly detection via blockchain deep learning smart contracts in industry 4.0. *Neural Comput Appl*. 2020 Sep 1; 32(23): 17361-78.
- [7] Bordel B, Alcarria R, Robles T. Lightweight encryption for short-range wireless biometric authentication systems in Industry 4.0. *Integr Comput-Aided Eng*. 2021 Jan 1; Preprint (Preprint): 1-21.
- [8] Ahmed M, Reno S, Akter N, Haque F. Securing Medical Forensic System Using Hyperledger Based Private Blockchain. In: *2020 23rd International Conference on Computer and Information Technology (ICCCIT)*. 2020. p. 1-6.
- [9] Demertzis K. Blockchain Federated Learning for Threat Defense. *ArXiv210212746; Cs [Internet]*. 2021 Feb 25 [cited 2022 Feb 16]; Available from: <http://arxiv.org/abs/2102.12746>.
- [10] Nassif AB, Talib MA, Nasir Q, Dakalbab FM. Machine Learning for Anomaly Detection: A Systematic Review. *IEEE Access*. 2021; 9: 78658-700.
- [11] Ferrag MA, Friha O, Maglaras L, Janicke H, Shu L. Federated Deep Learning for Cyber Security in the Internet of Things: Concepts, Applications, and Experimental Analysis. *IEEE Access*. 2021; 9: 138509-42.
- [12] Yousuf S, Svetinovic D. Blockchain Technology in Supply Chain Management: Preliminary Study. In: *2019 Sixth International Conference on Internet of Things: Systems, Management and Security (IOTSMS)*. 2019. p. 537-8.
- [13] Al Jallad K, Aljnidi M, Desouki MS. Anomaly detection optimization using big data and deep learning to reduce false-positive. *J Big Data*. 2020 Aug 31; 7(1): 68.
- [14] Jiang Z, Liu K. Real time interpretation and optimization of time series data stream in big data. In: *2018 IEEE 3rd International Conference on Cloud Computing and Big Data Analysis (ICCCBDA)*. 2018. p. 243-7.
- [15] Leal F, Veloso B, Malheiro B, Burguillo JC, Chis AE, González-Vélez H. Stream-based explainable recommendations via blockchain profiling. *Integr Comput-Aided Eng*. 2022 Jan 1; 29(1): 105-21.
- [16] Tellis VM, D'Souza DJ. Detecting Anomalies in Data Stream Using Efficient Techniques: A Review. In: *2018 International Conference on Control, Power, Communication and Computing Technologies (ICCPCT)*. 2018. p. 296-8.
- [17] Anderson TW. *An Introduction to Multivariate Statistical Analysis*. Wiley; 2003; 752 p.
- [18] Leung D, Romagnoli JA. Chapter 6.4 – Fault Diagnosis Methodologies for Process Operation. In: Braunschweig B, Gani R, editors. *Computer Aided Chemical Engineering [Internet]*. Elsevier; 2002 [cited 2022 Feb 16]. p. 535-56. (Software Architectures and Tools for Computer Aided Process Engineering; vol. 11). Available from: <https://www.sciencedirect.com/science/article/pii/S1570794602800244>.
- [19] Gawlikowski J, Tassi CRN, Ali M, Lee J, Humt M, Feng J, et al. A Survey of Uncertainty in Deep Neural Networks. *ArXiv210703342; Cs Stat [Internet]*. 2021 Jul 7 [cited 2021 Nov 6]; Available from: <http://arxiv.org/abs/2107.03342>.
- [20] Xue Y, Zhu H, Neri F. A self-adaptive multi-objective feature selection approach for classification problems. *Integr Comput-*

- 848 Aided Eng. 2022 Jan 1; 29(1): 3-21.
- 849 [21] Xu G, Li H, Liu S, Yang K, Lin X. VerifyNet: Secure and  
850 Verifiable Federated Learning. *IEEE Trans Inf Forensics Secur.*  
851 2020; 15: 911-26.
- 852 [22] Hua G, Zhu L, Wu J, Shen C, Zhou L, Lin Q. Blockchain-  
853 Based Federated Learning for Intelligent Control in Heavy  
854 Haul Railway. *IEEE Access.* 2020; 8: 176830-9.
- 855 [23] Liu H, Lang B, Chen S, Yuan M. Interpretable deep learning  
856 method for attack detection based on spatial domain attention.  
857 In: 2021 IEEE Symposium on Computers and Communica-  
858 tions (ISCC). 2021. p. 1-6.
- 859 [24] Ren C, Xu Y, Zhang R. An Interpretable Deep Learning  
860 Method for Power System Dynamic Security Assessment via  
861 Tree Regularization. *IEEE Trans Power Syst.* 2021; 1-1.
- 862 [25] Li D, Wang J, Tan Z, Li X, Hu Y. Differential Privacy Preser-  
863 vation in Interpretable Feedforward-Designed Convolutional  
864 Neural Networks. In: 2020 IEEE 19th International Confer-  
865 ence on Trust, Security and Privacy in Computing and Com-  
866 munications (TrustCom). 2020. p. 631-8.
- 867 [26] Petrosyan L, Sedakov A, Sun H, Xu G. Time consistency of the  
868 interval Shapley-like value in dynamic games. *J Intell Fuzzy*  
869 *Syst.* 2016 Jan 1; 30(4): 1965-72.
- 870 [27] Guo B, Hao S, Cao G, Gao H. Profit distribution of liner  
871 alliance based on shapley value. *J Intell Fuzzy Syst.* 2021 Jan  
872 1; 41(4): 5081-5.
- 873 [28] Freer C, Kjos-Hanssen BRM, Nies A, Stephan F. Algorithmic  
874 Aspects of Lipschitz Functions. *Computability.* 2014 Jan 1;  
875 3(1): 45-61.
- 876 [29] Gao Y, Jia L. Stability in measure for uncertain delay differ-  
877 ential equations based on new Lipschitz conditions. *J Intell*  
878 *Fuzzy Syst.* 2021 Jan 1; 41(2): 2997-3009.
- 879 [30] Rafiei MH, Adeli H. A New Neural Dynamic Classification  
880 Algorithm. *IEEE Trans Neural Netw Learn Syst.* 2017 Dec;  
881 28(12): 3074-83.
- 882 [31] Pereira DR, Piteri MA, Souza AN, Papa JP, Adeli H. FEMA: a  
883 finite element machine for fast learning. *Neural Comput Appl.*  
884 2020 May 1; 32(10): 6393-404.
- 885 [32] Demertzis K, Iliadis L, Kikiras P. A Lipschitz – Shapley Ex-  
886 plainable Defense Methodology Against Adversarial Attacks.  
887 In: Maglogiannis I, Macintyre J, Iliadis L, editors. *Artificial In-*  
888 *telligence Applications and Innovations AIAI 2021; IFIP WG*  
889 *125 International Workshops.* Cham: Springer International  
890 Publishing; 2021. p. 211-27. (IFIP Advances in Information  
891 and Communication Technology).
- 892 [33] Alam KMdR, Siddique N, Adeli H. A dynamic ensemble learn-  
893 ing algorithm for neural networks. *Neural Comput Appl.* 2020  
894 Jun 30; 32(12): 8675-90.
- 895 [34] Rafiei MH, Khushefati WH, Demirboga R, Adeli H. Super-  
896 vised Deep Restricted Boltzmann Machine for Estimation of  
897 Concrete. *Mater J.* 2017 Mar 1; 114(2): 237-44.
- 898 [35] Xing L, Demertzis K, Yang J. Identifying data streams anom-  
899 alies by evolving spiking restricted Boltzmann machines. *Neural*  
900 *Comput Appl.* 2020 Jun 1; 32(11): 6699-713.
- 901 [36] Lipovetsky S, Conklin WM. Meaningful regression analysis in  
902 adjusted coefficients Shapley value model. *Model Assist Stat*  
903 *Appl.* 2010 Jan 1; 5(4): 251-64.
- 904 [37] Meng F, Chen X, Zhang Q. Some uncertain generalized Shap-  
905 ley aggregation operators for multi-attribute group decision  
906 making. *J Intell Fuzzy Syst.* 2015 Jan 1; 29(4): 1251-63.
- 907 [38] Gąsienica-Józkowy J, Knapik M, Cyganek B. An ensemble  
908 deep learning method with optimized weights for drone-based  
909 water rescue and surveillance. *Integr Comput-Aided Eng.* 2021  
910 Jan 1; 28(3): 221-35.
- [39] Liapis S, Christantonis K, Chazan-Pantzalis V, Manos A, Eliz-  
911 abeth Filippidou D, Tjortjis C. A methodology using classifi-  
912 cation for traffic prediction: Featuring the impact of & nbsp;  
913 COVID-19. *Integr Comput-Aided Eng.* 2021 Jan 1; 28(4):  
914 417-35.
- [40] 8080labs. ppscore – a Python implementation of the Predic-  
915 tive Power Score (PPS) [Internet]. 2022 [cited 2022 Feb 16].  
916 Available from: <https://github.com/8080labs/ppscore>.  
917
- [41] Guopan S. The effect of probability on risk perception and risk  
918 preference in decision making. In: 2010 International Confer-  
919 ence on Education and Management Technology. 2010. p.  
920 690-3.
- [42] Peng P, Xie L, Wei H. A Deep Fourier Neural Network for  
921 Seizure Prediction Using Convolutional Neural Network and  
922 Ratios of Spectral Power. *Int J Neural Syst.* 2021 Aug; 31(8):  
923 2150022.
- [43] Gómez-Silva MJ, de la Escalera A, Armingol JM. Back-  
924 propagation of the Mahalanobis distance through a deep triplet  
925 learning model for person Re-Identification. *Integr Comput-*  
926 *Aided Eng.* 2021 Jan 1; 28(3): 277-94.
- [44] Wang Y, Sui M. Finite lattice approximation of infinite lattice  
927 systems with delays and non-Lipschitz nonlinearities. *Asymp-*  
928 *tot Anal.* 2018 Jan 1; 106(3-4): 169-203.
- [45] Cao S, Zhang G, Liu P, Zhang X, Neri F. Cloud-assisted secure  
929 eHealth systems for tamper-proofing EHR via blockchain. *Inf*  
930 *Sci.* 2019 Jun 1; 485: 427-40.
- [46] Xue Y, Zhang Q, Neri F. Self-Adaptive Particle Swarm  
931 Optimization-Based Echo State Network for Time Series Pre-  
932 diction. *Int J Neural Syst.* 2021 Dec; 31(12): 2150057.
- [47] Xue Y, Jiang P, Neri F, Liang J. A Multi-Objective Evolution-  
933 ary Approach Based on Graph-in-Graph for Neural Architec-  
934 ture Search of Convolutional Neural Networks. *Int J Neural*  
935 *Syst.* 2021 Sep; 31(9): 2150035.
- [48] Rafiei MH, Adeli H. NEEWS: A novel earthquake early warn-  
936 ing model using neural dynamic classification and neural dy-  
937 namic optimization. *Soil Dyn Earthq Eng.* 2017 Sep 1; 100:  
938 417-27.
- [49] Hassanpour A, Moradikia M, Adeli H, Khayami SR, Sham-  
939 sinejadbabaki P. A novel end-to-end deep learning scheme for  
940 classifying multi-class motor imagery electroencephalography  
941 signals. *Expert Syst.* 2019; 36(6): e12494.
- [50] DDoS 2019 | Datasets | Research | Canadian Institute for Cy-  
942 bersecurity | UNB [Internet]. [cited 2022 Feb 16]. Available  
943 from: <https://www.unb.ca/cic/datasets/ddos-2019.html>.  
944
- [51] Sharafaldin I, Lashkari AH, Hakak S, Ghorbani AA. Develop-  
945 ing Realistic Distributed Denial of Service (DDoS) Attack  
946 Dataset and Taxonomy. In: 2019 International Carnahan Con-  
947 ference on Security Technology (ICCST). 2019. p. 1-8.
- [52] Martins GB, Papa JP, Adeli H. Deep learning techniques for  
948 recommender systems based on collaborative filtering. *Expert*  
949 *Syst.* 2020; 37(6): e12647.
- [53] Rafiei MH, Adeli H. Novel Machine-Learning Model for Esti-  
950 mating Construction Costs Considering Economic Variables  
951 and Indexes. *J Constr Eng Manag.* 2018 Dec 1; 144(12):  
952 04018106.
- [54] Ahmadi M, Adeli H. Enhanced probabilistic neural network  
953 with local decision circles: A robust classifier. *Integr Comput-*  
954 *Aided Eng.* 2010 Jan 1; 17(3): 197-210.
- [55] Anezakis VD, Demertzis K, Iliadis L, Spartalis S. A Hybrid  
955 Soft Computing Approach Producing Robust Forest Fire Risk  
956 Indices. In: Iliadis L, Maglogiannis I, editors. *Artificial Intelli-*  
957 *gence Applications and Innovations.* Cham: Springer Interna-  
958 tional Publishing; 2016; p. 191-203.